

# DKiS: Decay weight invertible image steganography with private key

Hang Yang  
College of Science  
China Agricultural University  
Beijing 100083, China  
yanghang@cau.edu.cn

Yitian Xu  
College of Science  
China Agricultural University  
Beijing 100083, China  
xytshuxue@126.com

Xuhua Liu  
College of Science  
China Agricultural University  
Beijing 100083, China  
liuxuhua@cau.edu.cn

## Abstract

Image steganography, the practice of concealing information within another image, traditionally faces security challenges when its methods become publicly known. To counteract this, we introduce a novel private key-based image steganography technique. This approach ensures the security of hidden information, requiring a corresponding private key for access, irrespective of the public knowledge of the steganography method. We present experimental evidence demonstrating our method's effectiveness, showcasing its real-world applicability. Additionally, we identified a critical challenge in the invertible image steganography process: the transfer of non-essential, or 'garbage', information from the secret to the host pipeline. To address this, we introduced the decay weight to control the information transfer, filtering out irrelevant data and enhancing the performance of image steganography. Our code is publicly accessible at <https://github.com/yanghangAI/DKiS>, and a practical demonstration is available at <http://yanghang.site/hidekey>.

## 1. Introduction

Image steganography, a subset of the broader field of steganography, involves the practice of concealing information within a digital image [17, 20]. This technique is rooted in the ancient art of hidden communication, but has evolved significantly with the advent of digital technologies. At its core, image steganography aims to embed data, such as text, audio, or another image, into a host image in a manner that is undetectable to the casual observer [35]. The primary objective is to maintain the apparent normalcy of the host image while secretly carrying additional information.

The evolution of image steganography has been marked by various methods and technologies. Initially, simple techniques [7, 25] like the Least Significant Bit (LSB) insertion

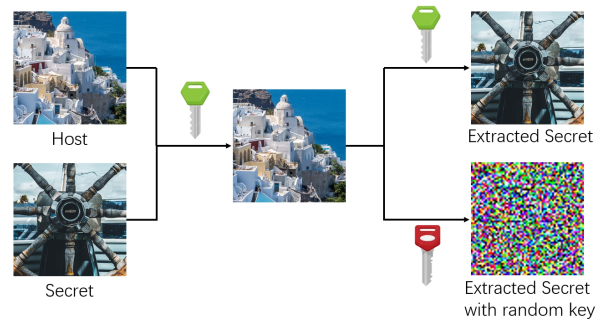


Figure 1. The workflow of image steganography with a private key.

were used, where information is embedded in the least significant bits of the pixel values of an image, causing minimal visual alteration [18]. Some other methods [6, 13] include transform domain techniques, where information is embedded in frequency domain of an image, making it more resilient to compression and other image processing operations.

The introduction of deep learning has further advanced the field of image steganography [5, 8–10, 24, 37]. By employing complex neural networks, it has become possible to embed larger amounts of data with improved security measures. These deep learning models can learn optimal ways to conceal data within images, making detection by third-party observers or automated systems significantly more challenging.

Image steganography continues to evolve, facing the challenge of maintaining confidentiality amidst widespread popularity. The known methods of steganography can be compromised by unauthorized parties, making it unsuitable for high-security contexts. To address this, our research integrates preset private keys into high-capacity image steganography, as shown in Fig. 1 based on invertible neural networks. This innovative approach secures the em-

bedded data even if the steganographic technique is widely known, using preset private keys that eliminate the need for transmission with the container image—thereby reducing interception risks. Our method, which combines advanced deep learning algorithms with this novel key management strategy, shows promising effectiveness in our experimental results. This highlights its potential for various applications, including secure communications and confidential data storage, where stringent security measures are paramount.

In addition, we find that when the information passing through the secret pipeline, the amount of secret part is getting less and less, which gives us the idea to limit the information transfer from secret pipeline into the host pipeline. Therefore we proposed the decay weight for a better performance.

The main contributions are listed as follows:

1. Preset private key is introduced into deep learning based image steganography for the first time, which extremely increase the security of image steganography.
2. Decay weight is proposed to control the amount of information transfer into the host pipeline from the secret pipeline based on the insight that the secret information is getting less and less as the secret pass through the secret pipeline.

## 2. Related Works

### 2.1. Image Steganography without Private Key

Image steganography is broadly categorized into traditional and deep learning-based methods.

**Traditional Image Steganography:** The most prevalent method in this category is the Least Significant Bit (LSB) technique [7, 32], which embeds secret messages by altering the  $n$  least significant bits of the host image. However, these modifications make it susceptible to detection by steganalysis methods [11, 12, 39]. Other notable techniques include Pan’s pixel value differencing (PVD) [27], Tsai’s histogram shifting [33], Nguyen’s use of multiple-bit-planes [26], and Imaizumi’s palette-based approach [14]. Some traditional methods utilize frequency domains like discrete cosine transform (DCT) [13], discrete Fourier transform (DFT) [28], and discrete wavelet transform (DWT) [6]. These methods offer more robustness and stealth than LSB techniques, though they still face limitations in payload capacity.

**Deep Learning-Based Image Steganography:** Recent advancements have seen deep learning techniques significantly outperform traditional methods in image steganography. HiDDeN [41] and SteganoGAN [38] utilize an encoder-decoder architecture, coupled with a third network to counteract steganalysis. Shi’s Ssgan [31] is based on generative adversarial networks. Baluja [4, 5] and Zhang

[37] have achieved higher payload capacities by hiding secret images of the same size as the host image. Lu [24], Jing [16], and Jia [15] have introduced invertible neural networks (INN) into the field and achieved SOTA performance in this area.

### 2.2. Image Steganography with Private Key

To address security issues arising from the widespread use of steganographic methods, researchers have proposed LSB-based image steganography utilizing private keys [2, 3, 19]. While this approach enhances security, it tends to suffer from low payload capacity. Seeking to increase capacity, Kweon [21] integrated private keys into a deep learning-based steganography framework. Although this method achieves higher capacities, it necessitates the transmission of the private key with the container image, which could potentially compromise security. Additionally, Kweon’s method faces low performance issues. The quality of generated image is not satisfied.

## 3. Method

### 3.1. Overview

The architecture of our DKiS model is illustrated in Fig. 2. In the embedding phase, the process involves the host image, secret image, and a private key as inputs, producing the container image and what we term as ‘missing info’. The term ‘missing info’ is used because, during transmission, only the container image is sent to the receiver, resulting in the missing of the other image. DKiS requires two images for both embedding and extraction phases. Consequently, a placeholder Gaussian distribution is introduced into DKiS alongside the container image and key. And the generated extracted image is indistinguishable from the original secret image if and only if the key used matches the one employed during the embedding phase.

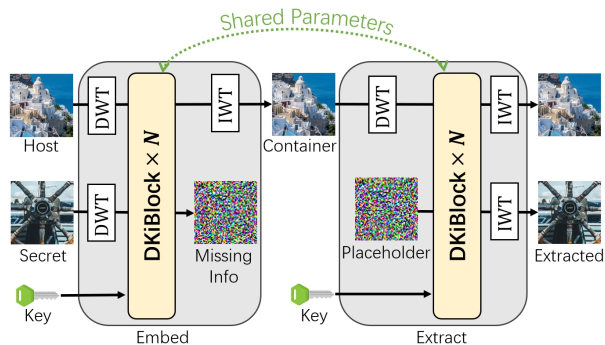


Figure 2. The overview of DKiS.

Additionally, before the host, secret, and container images are processed by the DKiBlocks, a discrete wavelet

transform (DWT) is applied to these input images. Correspondingly, an inverse discrete wavelet transform (IWT) is applied to the output from the DKiBlocks based on the work of [16].

### 3.2. DKiBlock

The architecture of the DKiBlock is depicted in Fig. 3. This design is founded on invertible blocks [34], enhanced through the incorporation of a decay weight and a private key.

$$\begin{aligned} x_k^{i+1} &= E(x_s^i, k_i) \\ x_h^{i+1} &= x_h^i + w_i \cdot f(x_k^i) \\ x_s^{i+1} &= x_k^i \otimes \exp(\sigma(g(x_h^{i+1}))) + h(x_h^{i+1}) \end{aligned} \quad (1)$$

With a little transformation of Eq. (1), the inverse processes is gained and shown as below:

$$\begin{aligned} x_k^i &= (x_s^{i+1} - h(x_h^{i+1})) \otimes \exp(-\sigma(g(x_h^{i+1}))) \\ x_h^i &= x_h^{i+1} - w \cdot f(x_k^i) \\ x_s^i &= E^-(x_k^{i+1}, k_i) \end{aligned} \quad (2)$$

Where  $E$  is the encode function, it encodes the input  $x$  with  $k$ , and in order to maintain the invertible ability, it needs to have invert function  $E^-$ , the detail of  $E$  will be shown in Section 3.4. And  $w_i$  is the decay weight, the detail and purpose will be discussed in Section 3.3.

### 3.3. Decay Weight

The extraction process becomes more challenging as the amount of secret information in ‘mission info’ increases. For optimal performance, it is crucial to minimize the information about the secret image in the ‘missing info’. Ideally, this ‘missing info’ should closely resemble the placeholder Gaussian distribution.

However, the transformation from secret image to ‘missing info’ is impossible to finish in one invertible block. To better understand this, we analyzed the outputs of the secret pipeline, as depicted in Fig. 4. We observed that the deviation of each  $x_s^i$  from the secret image increases with the increment of  $i$ . To quantify these deviations, we calculated the distances/similarity between the secret image and each  $x_s^i$ , employing metrics such as Average Pixel Distance (APD), Peak Signal-to-Noise Ratio (PSNR), and the Structural Similarity Index Model (SSIM), which are elaborated in Section 4.2. The comparative findings are displayed in Fig. 5. This analysis indicates a progressive divergence of  $x_s^i$  from the secret image with increasing  $i$ , signifying a reduction in the information content of the secret image as it progresses through the secret pipeline.

Recognizing that less information about the secret image reduces the necessity for its transmission into the host pipeline, we introduced a decay weight  $w_i$  to modulate the

amount of information transferred from the secret to the host pipeline. The formulation of  $w_i$  is detailed in Eq. 3, where  $r$  represents the decay rate.

$$w_i = r^i \quad (3)$$

### 3.4. Private Key

We have incorporated a private key into the secret pipeline through an encoding function,  $E(\cdot)$ , as illustrated in Fig. 6.

This encoding process comprises two main steps: shuffling and element-wise multiplication. The private key,  $k_i$ , is divided into two components:  $k_m^i$  and  $k_s^i$ . In the first step, the image is segmented into  $4 \times 4$  small patches (for clarity, Fig. 6 only displays  $2 \times 2$  patches). These patches are then shuffled according to the sequence determined by  $k_s^i$ . In the second step, the image undergoes element-wise multiplication by  $k_m^i$ . Here,  $k_m^i$  is of the same dimensions as  $x_s^i$ , and each element in  $k_m^i$  has an equal probability of being either -1 or 1. It is important to note that the encoding operation is invertible solely when the correct key is available.

**Key Generation Process:** To generate the key, any user-preset key is first transformed into a 256-bit number using SHA-256 encoding [22]. This encoded number is then converted into a random seed, which is subsequently used to generate both  $k_s$  and  $k_m$ .

### 3.5. Loss Function

Our study addresses two distinct types of similarity. Firstly, we examine the differences between the host image  $x_h$  and the container image  $x_c$ , referred to as the C-pair. Secondly, we consider the differences between the secret images  $x_s$  and the extracted images  $x_e$ , termed the S-pair. To quantify these differences, we introduce two specific loss functions,  $L_c$  and  $L_s$ , defined as follows:

$$L_c = \sum_p (x_c^{(p)} - x_h^{(p)})^2, \quad L_s = \sum_p (x_s^{(p)} - x_e^{(p)})^2 \quad (4)$$

In these equations,  $x^{(p)}$  denotes the pixel value at position  $p$  in image  $x$ . The terms  $L_c$  and  $L_s$  are designed to measure the similarities within the C-pair and S-pair, respectively. The overall loss function is then computed as a weighted sum of these two losses:

$$L = \lambda_c L_c + \lambda_s L_s \quad (5)$$

where  $\lambda_c$  and  $\lambda_s$  are weighting factors for the respective loss functions.

## 4. Experiment

### 4.1. Implementation Details

Unless otherwise specified, our model is trained on the DIV2K dataset [1]. We pre-process the input images by

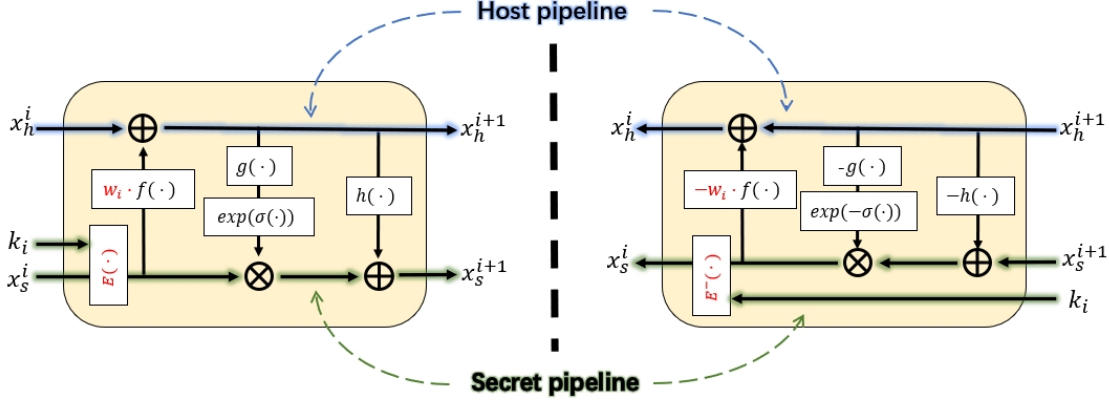


Figure 3. The architecture of DKiBlock. Left: forward process. Right: inverse process.

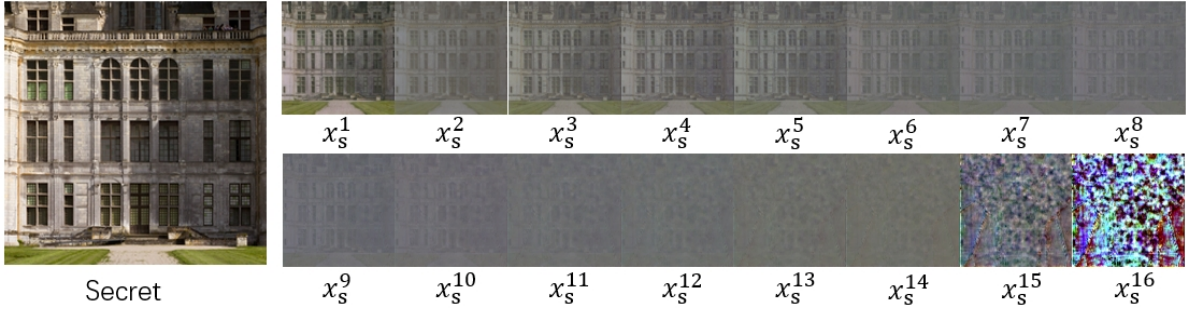


Figure 4. The outputs of secret pipeline.

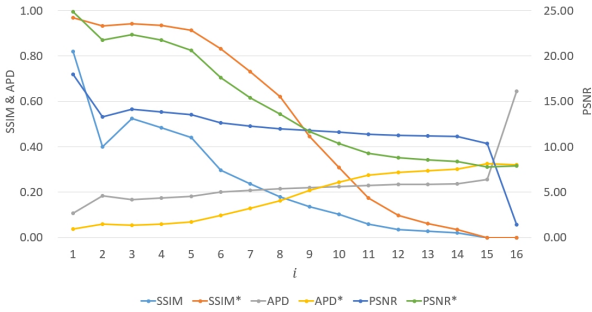


Figure 5. The SSIM, APD and PSNR values between each  $x_s^i$  and the secret image. \* denotes that  $x_s^i$  has been aligned to the secret image through a linear transformation. This alignment ensures that  $x_s^i$  matches the secret image in terms of mean and standard deviation.

cropping them to a resolution of  $256 \times 256$  pixels. To enhance generalization, we employ random cropping on the training dataset. Conversely, for the testing dataset, center cropping is utilized to eliminate randomness in evaluation. The weighting factors  $\lambda_c$  and  $\lambda_s$  are both set to 1. The training process involves 1600 epochs, utilizing the Adam optimizer with a learning rate of  $10^{-4.5}$ , and  $\beta_1 = 0.9$ ,  $\beta_2 = 0.99$ . The learning rate is halved every 200 epochs to



Figure 6. The overview of encode operation.

optimize convergence.

Acknowledging the inevitability of rounding errors in real-world applications, we incorporate a rounding operation on the container image in all our experiments to simulate this effect. To address the non-differentiable nature of the rounding operation, we employ the Gradient Approximation Function (GAF) as described in PRIS [36].

## 4.2. Evaluation Criteria

The primary goal of image steganography is to maximize similarity in the C-pair (container and host images) and the S-pair (secret and extracted images). Introducing a private key into our system, we define a new pair called the S'-pair, which consists of the secret image and an incorrectly extracted secret image using an incorrect key.

Our evaluation employs the Peak Signal-to-Noise Ratio (PSNR) and the Structural Similarity Index Model (SSIM) [30] to measure image similarity, with higher values indicating greater similarity. These metrics are denoted as PSNR- $x$  and SSIM- $x$ , where 'x' specifies the image pair under evaluation. For C-pair and S-pair, higher PSNR and SSIM values suggest superior steganographic performance. In contrast, lower PSNR and SSIM values for the S'-pair indicate enhanced security against unauthorized information extraction.

Additionally, we utilize the Average Pixel Distance (APD) for quantifying the pixel-wise distance between two images, as defined in 6. In this context,  $x^{(p)}$  and  $y^{(p)}$  represent pixel values of images  $x$  and  $y$  at position  $p$ , respectively, and  $N$  is the total number of pixels. A higher APD value implies a greater distance between the images.

$$APD(x, y) = \frac{1}{N} \sum_p |x^{(p)} - y^{(p)}| \quad (6)$$

### 4.3. Ablation Study

To illustrate the effectiveness of our proposed decay weight and standardize pre-process techniques, we conducted ablation studies. As shown in Table 1, the incorporation of decay weight and standardize pre-process with  $r = 0.6$  resulted in a significant improvement, reducing the loss value by 23.14%.

We conducted comparative analyses to evaluate the effects of implementing decay weights on the missing information in our model. These comparisons included scenarios without decay weight, with a decay weight characterized by  $r = 0.6$ , and with a Gaussian distribution. The results, as illustrated in Fig. 7, reveal that the introduction of the decay weight leads to a pattern of missing information that more closely aligns with that of the Gaussian distribution. This alignment provides insight into why the decay weight is effective in our model.

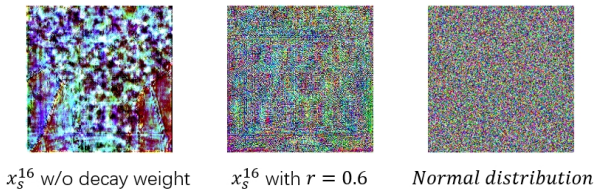


Figure 7. The comparison of the missing info of secret pipeline between without decay weight, with  $r = 0.6$  and Normal distribution.

### 4.4. Experiments with Private Key

Due to the novelty of our method, which involves hiding an image within another image using a private key, direct

comparisons with existing techniques are challenging. The most closely related work [21] operates under a significant constraint: the key is generated by embedding networks, and cannot be preset. This implies that the key must be transmitted alongside the container image, a limitation our method overcomes. Consequently, a direct, fair comparison with existing methods is not feasible. Despite the increased practicality and complexity of our task compared to previous work, our approach demonstrates superior performance, as evidenced by the results presented in Tab. 2 and Fig. 10.

We expanded our experimentation to include additional datasets, as summarized in Tab. 3. We incorporated a subset of the COCO-2017 dataset [23], selecting 6,000 images at random, to evaluate our model's performance on diverse real-world scenarios. Additionally, we used a set of 1,000 images from the ImageNet-2012 [29] to further assess the model's robustness in varied photographic contexts. Furthermore, to test the model's applicability in a different domain, we employed a sample of 1,000 images from PubLayNet [40], a dataset only consisting of document images, contrasting the real-world photos in the other datasets. The consistent performance across these varied datasets underscores the versatility and adaptability of our method in handling both photographic and document imagery.

### 4.5. How is the secret image hiding?

To illustrate how the secret image is concealed, we analyzed the differences between host and container images, as depicted in Fig. 8. The first row displays the secret images. The second and third rows show the differences between C-pair without and with the private key, respectively. Since these differences are typically visually undetectable, we enhanced the images in the last two rows for clearer visualization. This enhancement involved multiplying the differences by a factor of 10 and increasing the brightness by 40%.

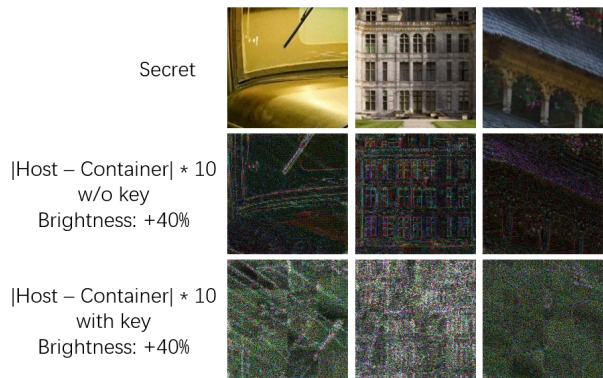


Figure 8. The difference between host and container images.

The first two rows exhibit similar patterns, suggesting

Table 1. Ablation studies for normal pre-process and decay rate.

Pre-process	Decay rate	PSNR-C $\uparrow$	PSNR-S $\uparrow$	SSIM-C $\uparrow$	SSIM-S $\uparrow$	Loss $\downarrow$
Normalize	$\times$	40.63	40.39	.9928	.9987	42.65
Standardize	$\times$	41.40	41.11	.9945	.9989	35.41
Standardize	0.9	41.25	41.21	.9945	.9989	35.77
Standardize	0.8	41.49	41.21	.9947	.9989	34.88
Standardize	0.7	41.73	41.43	.9946	.9990	32.78
Standardize	0.6	<b>41.91</b>	<b>41.62</b>	<b>.9948</b>	<b>.9990</b>	<b>31.48</b>
Standardize	0.5	41.54	40.97	.9943	.9989	36.05

Table 2. Results with private key.

Method	PSNR-C $\uparrow$	PSNR-S $\uparrow$	SSIM-C $\uparrow$	SSIM-S $\uparrow$	PSNR-S' $\downarrow$	SSIM-S' $\downarrow$
Kweon [21]	22.73	26.39	.9485	.9859	11.52	.4109
Our	36.04	31.95	.9858	.9906	8.71	.0014

Table 3. Experiment results on other datasets.

Dataset	PSNR-C $\uparrow$	PSNR-S $\uparrow$	SSIM-C $\uparrow$	SSIM-S $\uparrow$	PSNR-S' $\downarrow$	SSIM-S' $\downarrow$
DIV	36.04	31.95	.9858	.9906	8.66	.0000
COCO	32.92	30.33	.9938	.9886	8.49	.0000
ImageNet	33.25	31.01	.9950	.9900	8.32	.0002
PubLayNet	36.88	27.25	.9969	.9764	10.84	.0000

that the secret image is embedded in the host image through a specific addition operation. However, with the introduction of a private key, these shared patterns are no longer evident. This indicates that the private key modifies the embedding process with a more complicated way, thereby enhancing the security of the embedded image.

## 5. Application

The integration of a private key significantly enhances the security of image hiding techniques, particularly for methods that are publicly accessible. For example, the use of a private key enables our method to address challenges that traditional image hiding approaches cannot solve. For instance, consider the application in photo verification. As illustrated in Fig. 9, camera manufacturers can embed a secret verification image into photos using a private key known only to them. If verification is required, users can submit the photo to the manufacturer. Successful extraction of the secret verification image by the manufacturer will confirm that the photo was taken with their product and has not been modified. This approach could become a universal standard among camera manufacturers, with each set-

ting their unique private key. In the event of a key leak, the impact would be limited to the compromised manufacturer, while the integrity of other cameras remains unaffected.

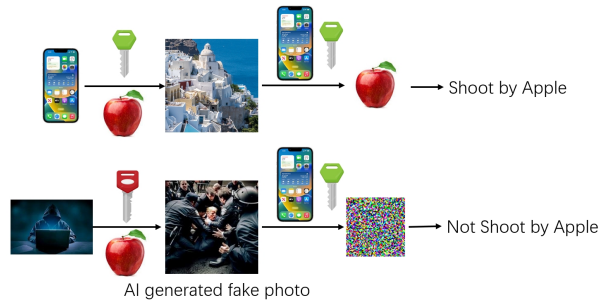


Figure 9. Photo verification.

## 6. Conclusion

In this paper, we introduced DKiS, a pioneering approach in the realm of image steganography, distinguished by its integration of a private key mechanism. Central to DKiS is the novel concept of decay weight, which strate-

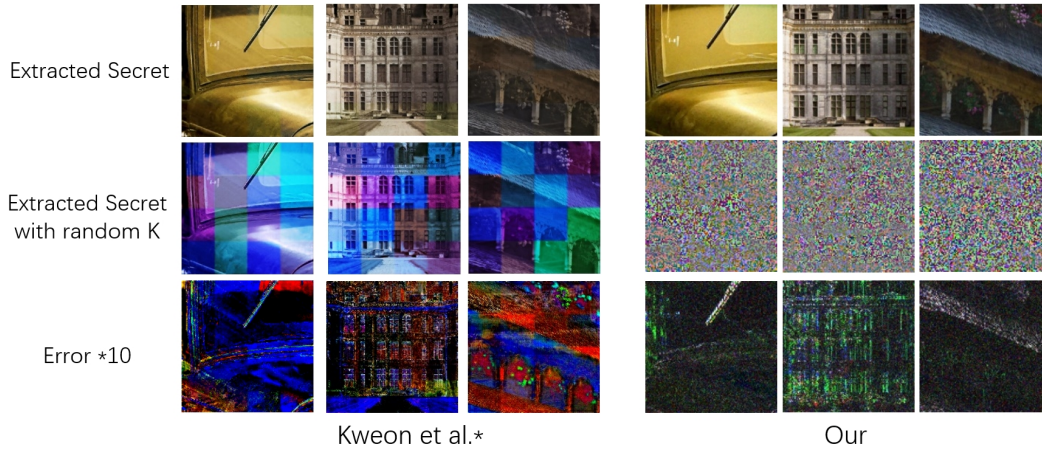


Figure 10. Visual comparison.

gically controls the transfer of information from the secret pipeline to the host pipeline. This is based on the insight that the relevance of information for the host pipeline diminishes progressively along the secret pipeline. The implementation of decay weight has notably enhanced the overall performance of the method.

A pivotal feature of DKiS is the incorporation of a private key into the steganographic process. This addition effectively addresses the longstanding challenge of balancing widespread accessibility with robust security in image steganography. As a result, DKiS emerges as a viable candidate for standardization in applications like image verification, where both the publicity and security of steganographic methods are paramount.

Our extensive experimental evaluations, conducted under conditions that include rounding errors, affirm the satisfactory performance of DKiS. The results demonstrate not only the method's efficacy in securely hiding images but also its potential as a versatile tool in a wide range of practical scenarios. DKiS, therefore, stands as a significant contribution to the field of image steganography, bridging the gap between public accessibility and stringent security requirements.

## References

- [1] Agustsson, E., Timofte, R.: Ntire 2017 challenge on single image super-resolution: Dataset and study. In: Proceedings of the IEEE conference on computer vision and pattern recognition workshops. pp. 126–135 (2017) [3](#)
- [2] Al-Husainy, M.A.F., Uliyan, D.M.: A secret-key image steganography technique using random chain codes. *International Journal of Technology* **10**(4), 731–740 (2019) [2](#)
- [3] Almazaydeh, W.I.A., Sheshadri, H.: Image steganography using a dynamic symmetric key. In: 2018 2nd International Conference on Trends in Electronics and Informatics (ICOEI). pp. 1507–1513. IEEE (2018) [2](#)
- [4] Baluja, S.: Hiding Images in Plain Sight: Deep Steganography (2017) [2](#)
- [5] Baluja, S.: Hiding images within images. *IEEE transactions on pattern analysis and machine intelligence* **42**(7), 1685–1697 (2019) [1](#), [2](#)
- [6] Barni, M., Bartolini, F., Piva, A.: Improved wavelet-based watermarking through pixel-wise masking. *IEEE transactions on image processing* **10**(5), 783–791 (2001) [1](#), [2](#)
- [7] Chan, C.K., Cheng, L.M.: Hiding data in images by simple lsb substitution. *Pattern recognition* **37**(3), 469–474 (2004) [1](#), [2](#)
- [8] Duan, X., Gou, M., Liu, N., Wang, W., Qin, C.: High-capacity image steganography based on improved xception. *Sensors* **20**(24), 7253 (2020) [1](#)
- [9] Duan, X., Jia, K., Li, B., Guo, D., Zhang, E., Qin, C.: Reversible image steganography scheme based on a u-net structure. *IEEE Access* **7**, 9314–9323 (2019) [1](#)
- [10] Duan, X., Nao, L., Mengxiao, G., Yue, D., Xie, Z., Ma, Y., Qin, C.: High-capacity image steganography based on improved fc-densenet. *IEEE Access* **8**, 170174–170182 (2020) [1](#)
- [11] Fridrich, J., Goljan, M., Du, R.: Detecting lsb steganography in color, and gray-scale images. *IEEE multimedia* **8**(4), 22–28 (2001) [2](#)
- [12] Hawi, T.A., Qutayri, M., Barada, H.: Steganalysis attacks on stego-images using stego-signatures and statistical image properties. In: 2004 IEEE Region 10 Conference TENCON 2004. pp. 104–107. IEEE (2004) [2](#)
- [13] Hsu, C.T., Wu, J.L.: Hidden digital watermarks in images. *IEEE Transactions on image processing* **8**(1), 58–68 (1999) [1](#), [2](#)
- [14] Imaizumi, S., Ozawa, K.: Multibit embedding algorithm for steganography of palette-based images. In: Image and Video Technology: 6th Pacific-Rim Symposium, PSIVT 2013, Guanajuato, Mexico, October 28–November 1, 2013. Proceedings 6. pp. 99–110. Springer (2014) [2](#)
- [15] Jia, X., Xin, H., Gu, L., Wang, H., Sun, J., Wan, W.: Afcihnet: Attention feature-constrained network for single image information hiding. *Engineering Applications of Artificial Intelligence* **126**, 107105 (2023) [2](#)
- [16] Jing, J., Deng, X., Xu, M., Wang, J., Guan, Z.: Hinet: Deep image hiding by invertible network. In: Proceedings of the IEEE/CVF International Conference on Computer Vision. pp. 4733–4742 (2021) [2](#), [3](#)
- [17] Johnson, N.F., Jajodia, S.: Exploring steganography: Seeing the unseen. *Computer* **31**(2), 26–34 (2 1998) [1](#)
- [18] Kadhim, I.J., Premaratne, P., Vial, P.J., Halloran, B.: Comprehensive survey of image steganography: Techniques, evaluations, and trends in future research. *Neurocomputing* **335**, 299–326 (2019) [1](#)
- [19] Karim, S.M., Rahman, M.S., Hossain, M.I.: A new approach for lsb based image steganography using secret key. In: 14th international conference on computer and information technology (ICCI 2011). pp. 286–291. IEEE (2011) [2](#)
- [20] Kessler, G.C., Hosmer, C.: An Overview of Steganography, pp. 51–107. Elsevier (2011) [1](#)
- [21] Kweon, H., Park, J., Woo, S., Cho, D.: Deep multi-image steganography with private keys. *Electronics* **10**(16), 1906 (2021) [2](#), [5](#), [6](#)
- [22] Lilly, G.M.: Device for and method of one-way cryptographic hashing (Dec 7 2004), uS Patent 6,829,355 [3](#)
- [23] Lin, T., Maire, M., Belongie, S.J., Bourdev, L.D., Girshick, R.B., Hays, J., Perona, P., Ramanan, D., Doll'ar, P., Zitnick, C.L.: Microsoft COCO: common objects in context. *CoRR* **abs/1405.0312** (2014), <http://arxiv.org/abs/1405.0312> [5](#)
- [24] Lu, S.P., Wang, R., Zhong, T., Rosin, P.L.: Large-capacity image steganography based on invertible neural networks. In: Proceedings of the IEEE/CVF Conference on Computer Vision and Pattern Recognition. pp. 10816–10825 (2021) [1](#), [2](#)



- [25] Luo, W., Huang, F., Huang, J.: Edge adaptive image steganography based on lsb matching revisited. *IEEE Transactions on information forensics and security* **5**(2), 201–214 (2010) [1](#)
- [26] Nguyen, B.C., Yoon, S.M., Lee, H.K.: Multi bit plane image steganography. In: *Digital Watermarking: 5th International Workshop, IWDW 2006, Jeju Island, Korea, November 8-10, 2006. Proceedings 5*. pp. 61–70. Springer (2006) [2](#)
- [27] Pan, F., Li, J., Yang, X.: Image steganography method based on pvd and modulus function. In: *2011 International Conference on Electronics, Communications and Control (ICECC)*. pp. 282–284. IEEE (2011) [2](#)
- [28] Ruanaidh, J., Dowling, W.J., Boland, F.M.: Phase watermarking of digital images. In: *Proceedings of 3rd IEEE International Conference on Image Processing*. vol. 3, pp. 239–242. IEEE (1996) [2](#)
- [29] Russakovsky, O., Deng, J., Su, H., Krause, J., Satheesh, S., Ma, S., Huang, Z., Karpathy, A., Khosla, A., Bernstein, M., Berg, A.C., Fei-Fei, L.: ImageNet Large Scale Visual Recognition Challenge. *International Journal of Computer Vision (IJCV)* **115**(3), 211–252 (2015). <https://doi.org/10.1007/s11263-015-0816-y> [5](#)
- [30] Setiadi, D.R.I.M.: Psnr vs ssim: imperceptibility quality assessment for image steganography. *Multimedia Tools and Applications* **80**(6), 8423–8444 (2021) [5](#)
- [31] Shi, H., Dong, J., Wang, W., Qian, Y., Zhang, X.: Ssgan: Secure steganography based on generative adversarial networks. In: *Advances in Multimedia Information Processing–PCM 2017: 18th Pacific-Rim Conference on Multimedia, Harbin, China, September 28-29, 2017, Revised Selected Papers, Part I 18*. pp. 534–544. Springer (2018) [2](#)
- [32] Tamimi, A.A., Abdalla, A.M., Al-Allaf, O.: Hiding an image inside another image using variable-rate steganography. *International Journal of Advanced Computer Science and Applications (IJACSA)* **4**(10) (2013) [2](#)
- [33] Tsai, P., Hu, Y.C., Yeh, H.L.: Reversible image hiding scheme using predictive coding and histogram shifting. *Signal processing* **89**(6), 1129–1143 (2009) [2](#)
- [34] Xiao, M., Zheng, S., Liu, C., Wang, Y., He, D., Ke, G., Bian, J., Lin, Z., Liu, T.Y.: Invertible image rescaling. In: *Computer Vision–ECCV 2020: 16th European Conference, Glasgow, UK, August 23–28, 2020, Proceedings, Part I 16*. pp. 126–144. Springer (2020) [3](#)
- [35] Xu, Y., Mou, C., Hu, Y., Xie, J., Zhang, J.: Robust invertible image steganography. In: *Proceedings of the IEEE/CVF Conference on Computer Vision and Pattern Recognition*. pp. 7875–7884 (2022) [1](#)
- [36] Yang, H., Xu, Y., Liu, X., Ma, X.: Pris: Practical robust invertible network for image steganography. *arXiv preprint arXiv:2309.13620* (2023) [4](#)
- [37] Zhang, C., Benz, P., Karjauv, A., Sun, G., Kweon, I.S.: Udh: Universal deep hiding for steganography, watermarking, and light field messaging. *Advances in Neural Information Processing Systems* **33**, 10223–10234 (2020) [1](#), [2](#)
- [38] Zhang, K.A., Cuesta-Infante, A., Xu, L., Veeramachani, K.: Steganogan: High capacity image steganography with gans. *arXiv preprint arXiv:1901.03892* (2019) [2](#)
- [39] Zhi, L., Fen, S.A., Xian, Y.Y.: A lsb steganography detection algorithm. In: *14th IEEE Proceedings on Personal, Indoor and Mobile Radio Communications, 2003. PIMRC 2003*. vol. 3, pp. 2780–2783. IEEE (2003) [2](#)
- [40] Zhong, X., Tang, J., Yepes, A.J.: Publaynet: largest dataset ever for document layout analysis. In: *2019 International Conference on Document Analysis and Recognition (ICDAR)*. pp. 1015–1022. IEEE (Sep 2019). <https://doi.org/10.1109/ICDAR.2019.00166> [5](#)
- [41] Zhu, J., Kaplan, R., Johnson, J., Fei-Fei, L.: Hidden: Hiding data with deep networks. In: *Proceedings of the European conference on computer vision (ECCV)*. pp. 657–672 (2018) [2](#)